Modelling the non-thermal X-ray emission of pulsars from their multi-wavelength pulse profiles

J. Pétri S. Guillot L. Guillemot D. Mitra M. Kerr L. Kuiper G. Theureau I. Cognard

CNRS, Observatoire astronomique de Strasbourg, France
IRAP, CNRS, Toulouse, France
LPC2E, Orléans, France
National Centre for Radio Astrophysics, India
Space Science Division, Naval Research Laboratory, Washington, DC 20375-5352, USA
SRON-Netherlands Institute for Space Research, Leiden, The Netherlands

XMM-Newton Workshop - 5th June 2024

Université de Strasbourg

Observatoire astronomique de Strasbourg

CEFIPRA

PROJET FINANCÉ PAR L'ANR - PROJECT FUNDED BY THE ANR

Summary

Objectives & Methods

Objectives of the study

- constrain the geometry of the pulsar and observer line of sight.
- identify the radio, X-ray and γ-ray emission mechanisms.
- localize the associated photon production sites.

Methods

- use young radio-loud γ-ray pulsar light-curves.
- radio emission altitude and angle constrained by RVM model.
- γ-ray emission from the striped wind.

Resuts

- Fitting jointly RVM model and γ-ray light-curves to find consistent radio and γ-ray geometries.
- localisation of the non-thermal X-ray emission height and radiation mechanism identification.

Possible sites for pulsed emission

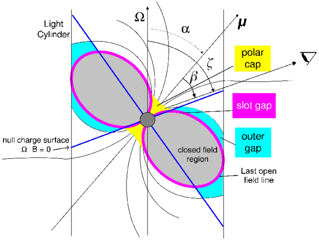

Figure – Emission models (Credit : Breed et al.).

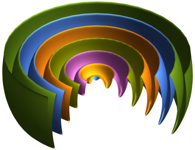

Figure – Pulsar striped wind current sheet.

Basic picture

- magnetosphere filled with $e^{\pm}$ plasma corotating with the neutron star up to the light-cylinder.
- corotation charge $\rho_{\rm GJ} = -2\,\varepsilon_0\,\vec{\Omega}\cdot\vec{B}$.
- no acceleration in regions where $\rho = \rho_{\rm GJ}$ because $E_{\parallel} = 0$.
- but acceleration in regions where $\rho \neq \rho_{\rm GJ}$ because $E_{\parallel} \neq 0$.

Four important sites

- polar cap : star surface R.
- slot gap : from R to $r_{\rm L}$.
- outer gap : from null-line to $r_{\rm L}$.
- striped wind : outside $r_{\rm L}$.

Emission model

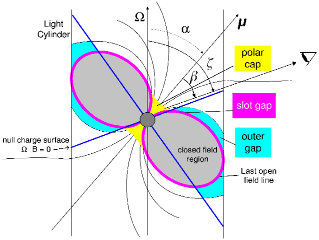

Figure – Emission models.

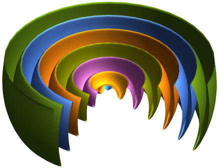

Figure – Pulsar striped wind current.

Essentially two parameters to fit

1. magnetic dipole inclination α.
2. observer line of sight inclination ζ $(= \alpha + \beta)$.

Computation of radio, X-ray and γ-ray pulse profile depending on α and ζ.

Radio atlas (polar cap) depending on $\{\alpha, \zeta\}$

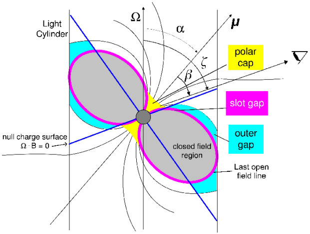

Figure – Radio photons coming from the polar cap region (yellow region).

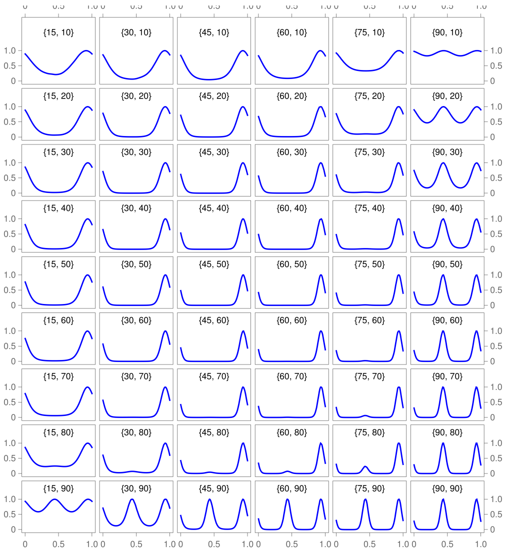

Atlas of radio pulse profiles for $\alpha = \{15°, 30°, 45°, 60°, 75°, 90°\}$ from left to right column and $\zeta = \{0°, ..., 90°\}$ in steps of $10°$ in the format $\{\alpha, \zeta\}$.

X-ray atlas (slot gap) depending on $\{\alpha, \zeta\}$

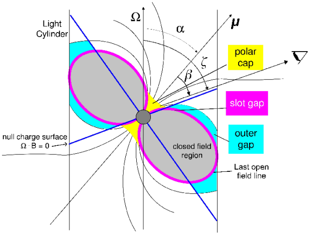

Figure – X-ray photons coming from the slot cap region (magenta region).

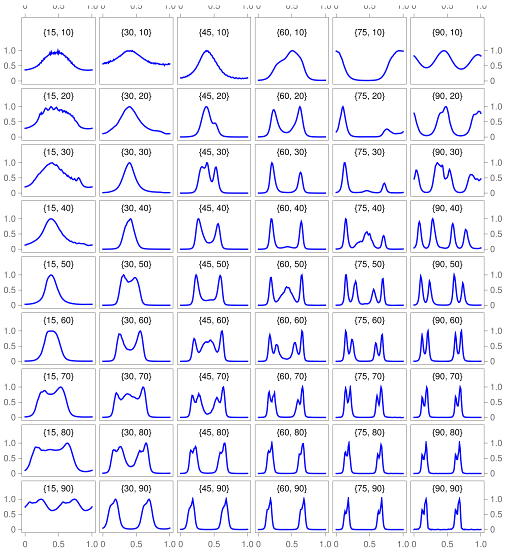

X-ray light curves for $\alpha = \{15^\circ, 30^\circ, 45^\circ, 60^\circ, 75^\circ, 90^\circ\}$ from left to right column and $\zeta = \{0^\circ, ..., 90^\circ\}$ in steps of 10° in the format $\{\alpha, \zeta\}$.

γ-ray atlas (striped wind) depending on $\{\alpha, \zeta\}$

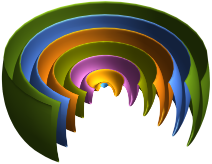

Figure – γ-ray photons coming from the striped wind (outside the magnetosphere).

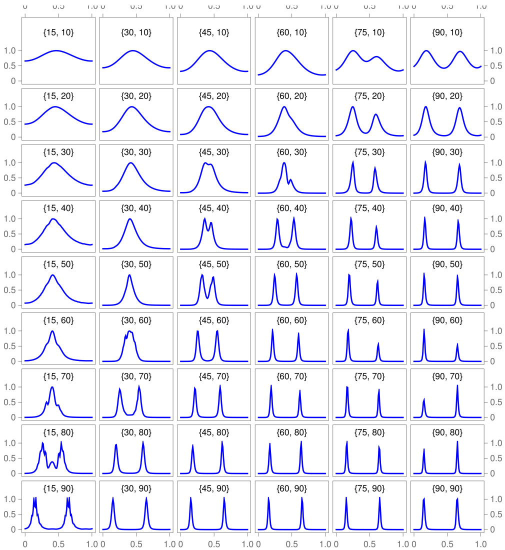

Atlas of γ-ray light curves for $\alpha = \{15°, 30°, 45°, 60°, 75°, 90°\}$ from left to right column and $\zeta = \{0°, ..., 90°\}$ in steps of $10°$ in the format $\{\alpha, \zeta\}$.

Fitting method

The χ^2 method

- compare theoretical γ-ray pulse profiles I^{model} to observations I^{obs}.
- uncertainties in measurements σ_{i}.
- minimizing the function χ^2_{n-1} summed on the binned data i

$$\chi^2_{n-1} = \frac{1}{n-1} \sum_{i=1}^{n} \frac{\left(I_{\mathrm{i}}^{\mathrm{obs}} - I_{\mathrm{i}}^{\mathrm{model}}\right)^2}{\sigma_{\mathrm{i}}^2} \tag{1}$$

Three parameters to fit

1. magnetic obliquity α.
2. line of sight inclination $\zeta = \alpha + \beta$.
3. phase shift between radio and γ-ray

$\Rightarrow$ simulates fluctuations in radio emission height or non radial beaming.

See Benli et al. (2021) and Pétri & Mitra (2021).

PSR J2229+6114 : non thermal X-ray fitting

Strategy

- find the angles (α, ζ) from joint radio and γ-ray.
- a good fit given by $(\alpha, \zeta) = (45°, 38°)$.
- adjust the X-ray emission site to fit the X-ray pulse profile.

Observations and results

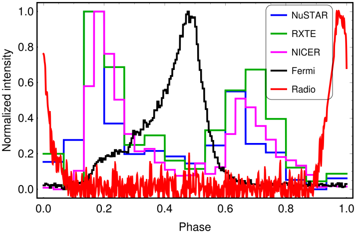

Figure – Multi-λ pulse profiles.

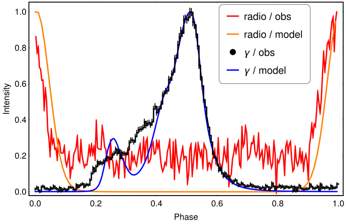

Figure – Joint radio and γ-ray fit.

PSR J2229+6114 : non-thermal X-ray fitting.

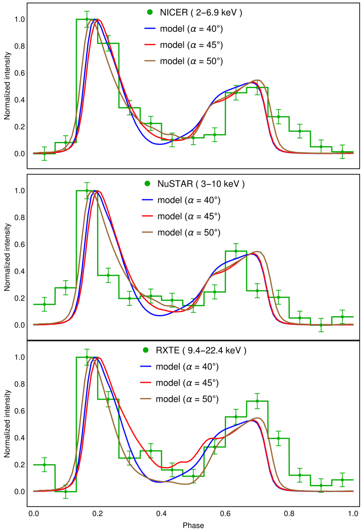

Figure – Fitted light-curves in X-ray.

Deduced parameters for good fits

	α	ζ	χ^2_ν
NICER	45	46	1.41
(1–10 keV)	50	32	1.17
RXTE	45	48	1.73
(9.4–22.4 keV)	50	34	1.83
NuSTAR	45	48	3.03
(3–10 keV)	50	48	1.65

Emission geometry

- emission height in $r/r_{\rm L} \in [0.2, 0.55]$.
- line of sight inclination agrees with γ-ray fit $\zeta \in [34°, 48°]$.

Pétri et al. (2024), in Press

Emission mechanism : energetics

Synchrotron vs curvature radiation

- synchrotron with $\gamma_{\rm syn} \approx 200$? $\Rightarrow$ secondary plasma.
- curvature with $\gamma_{\rm curv} \approx 10^5$? $\Rightarrow$ primary beam.

If curvature for radio and X-ray then

$$\frac{\gamma_{\rm X}}{\gamma_{\rm radio}} = \left(\frac{1 \text{ keV}}{1 \text{ GHz}\, h} \right)^{1/3} \approx 623$$

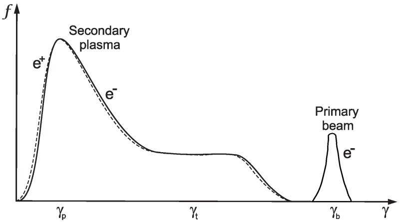

Figure – Primary and secondary beam distribution functions (Chkheidze, 2022).

Conclusions & Perspectives

Results of time-aligned radio/X-ray/γ-ray pulse profiles

- very efficient to constrain the geometry of the magnetic dipole.
- radio polarization reduces even more the uncertainties.
- non-thermal X-ray emission site between radio and γ-ray.
- determination of non-thermal X-ray emission altitude and extension.

Perspectives

- search for other good candidates seen in radio/X-ray/γ-ray.
- compute non-thermal X-ray spectra.

THANK YOU

FOR YOUR

ATTENTION

References

Benli O., Pétri J., Mitra D., 2021, A&A, 647, A101, publisher : EDP Sciences

Chkheidze N., 2022, Galaxies, 10, 59, number : 2 Publisher : Multidisciplinary Digital Publishing Institute

Pétri J., Guillot S., Guillemot L., Mitra D., Kerr M., Kuiper L., Cognard I., Theureau G., 2024, Localisation of the non-thermal X-ray emission of PSR~J2229+6114 from its multi-wavelength pulse profiles. ArXiv :2406.01244 [astro-ph]

Pétri J., Mitra D., 2021, A&A, 654, A106